Integration of orbital angular momentum in optical coherence tomography

Narag, Jadze Princeton; Adam, Aurèle J.L.

DOI
10.1051/epjconf/202533503025

Licence
CC BY

Publication date
2025

Document Version
Final published version

Published in
EPJ Web of Conferences

Citation (APA)
Narag, J. P., & Adam, A. J. L. (2025). Integration of orbital angular momentum in optical coherence tomography. *EPJ Web of Conferences*, *335*, Article 03025. https://doi.org/10.1051/epjconf/202533503025

Integration of orbital angular momentum in optical coherence tomography

Jadze Princeton Narag[1], and *Aurèle J.L.* Adam[1*]

[1]Optics Cluster Imaging Physics Department, Faculty of Applied Science, Delft University of Technology, Lorentzweg 1, 2628 CJ Delft, The Netherlands

Abstract. Optical Coherence Tomography (OCT) is a widely used non-invasive imaging technique, particularly in ophthalmology, offering high-resolution cross-sectional images of biological tissues. However, traditional OCT faces limitations in penetration depth and sensitivity, especially in highly scattering tissues. This work explores the integration of orbital angular momentum (OAM) with classical OCT. We demonstrate the generation of high-purity OAM modes in an OCT-compatible setup. The purity of these modes was evaluated through phase retrieval and OAM spectrum decomposition. While the use of a broadband source results in a reduction of mode purity, the dominant component remains the correctly generated OAM mode. Our preliminary results suggest the potential for using OAM as an additional degree of freedom in OCT, with applications for noise filtering and resolution enhancement. Furthermore, this approach could be extended to quantum OCT, where OAM entanglement is naturally integrated into the spontaneous parametric down-conversion (SPDC) process for photon generation.

1 Optical Coherence tomography

Optical Coherence Tomography (OCT) is a non-invasive imaging technique that provides high-resolution cross-sectional images of biological tissues. It is particularly valuable in ophthalmology for retinal imaging [1]. OCT relies on the principle of low-coherence interferometry, where a beam of light is split into two paths: one directed toward the tissue and the other serving as a reference. While classical OCT has revolutionized biomedical imaging, it faces limitations such as reduced penetration depth in highly scattering tissues and motion artifacts that hinder dynamic imaging [2].

Quantum OCT (QOCT) leverages quantum correlations to address some of these limitations, offering enhanced resolution and noise resilience using entangled photon pairs and coincidence detection techniques [3]. In QOCT, entangled photon pairs are typically generated via spontaneous parametric down-conversion (SPDC) [4,5]. One photon from each pair (the signal) interacts with the sample, while the other (the idler) travels along a reference path. A coincidence detector registers simultaneous photon arrivals, enabling depth-resolved imaging.

* Corresponding author: a.j.l.adam@tudelft.nl

Importantly, SPDC can produce photon pairs that are entangled not only in energy and time but also in orbital angular momentum (OAM) [5]. This additional degree of freedom may provide robustness against noise and act as a filter to improve imaging signal in QOCT systems [4-6]. Although OAM has been explored in various imaging modalities—such as enhancing penetration in scattering media [7] and improving resolution in STED microscopy [8]—its application to OCT, both classical and quantum, remains underexplored.

In our work, we investigate the role of OAM in the context of classical OCT. We present preliminary results demonstrating the generation of OAM states from a low-coherence source and characterize the OAM spectrum after the beam passes through a scattering sample. At the time of the conference, we aim to present OCT results using an OAM-encoded incident beam.

2 Generation of OAM for OCT

Our OCT setup incorporating OAM is illustrated in Figure 1. The light source can be either a laser (for alignment and testing) or a low-coherence LED source (for actual OCT measurements). The beam is first shaped and collimated using a spatial filter (SF). Its polarization is then controlled with a polarizer (P) and a half-wave plate (HWP) to match the modulation axis of the spatial light modulator (SLM).

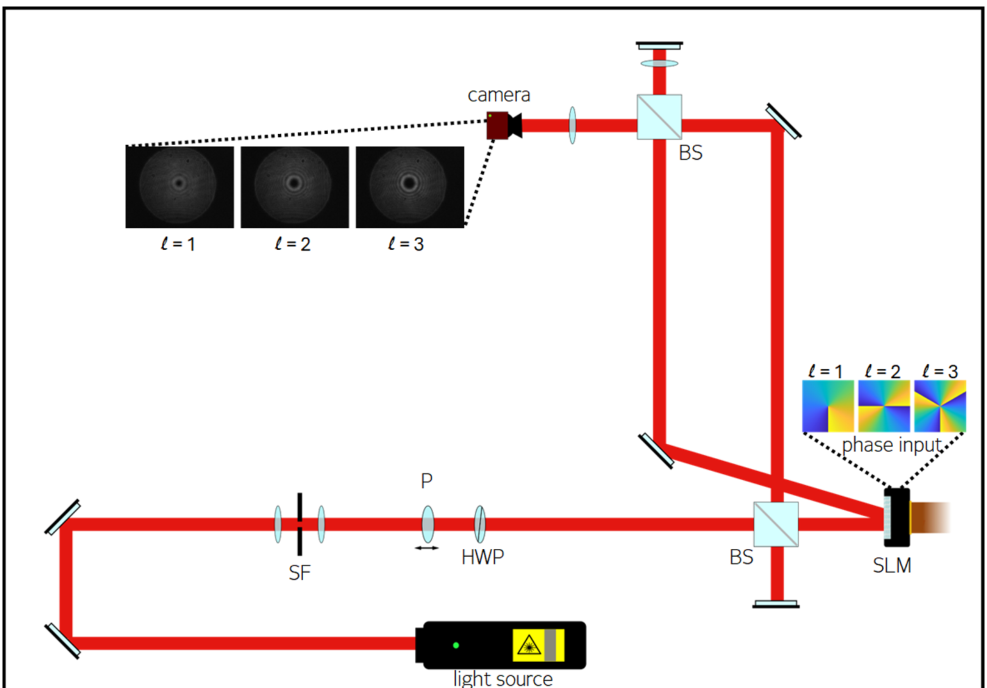

Fig. 1. OCT setup with OAM generation. Light from a laser or LED is collimated, polarization-adjusted, and split into two arms. One arm passes through an SLM to generate OAM modes; the other reflects off a mirror. The beams are recombined, and interference is captured by a camera. Inset: phase mask on the SLM.

The beam is split into two paths using a beam splitter (BS). One path is directed toward the SLM, where a helical phase pattern is imparted to generate an OAM mode. The phase mask used on the SLM is shown in the inset of Figure 1. The second path serves as the reference arm and is reflected off a mirror. After passing through their respective arms, the signal and reference beams are recombined at the beam splitter. The resulting interference pattern is captured by a camera, enabling characterization of the generated OAM modes and forming the basis for OCT measurements.

3 Results and Discussions

The generated OAM beams, captured by the camera, are shown in Figures 2(a)–2(c) for ℓ=1,2,3. The phase of these beams, also shown in Figures 2(a)–(c), was recovered using a 5-step interferometric phase retrieval method. By analyzing the helicity of the recovered phases, we can confirm that the generated OAM beams correspond to the expected ℓ values. To assess the purity of these modes, we decomposed the beams into their OAM spectrum, as shown in the corresponding bar graphs. The graphs demonstrate high purity for the modes ℓ=1,2,3. Figures 2(d)–(e) show the OAM spectrum spanning ℓ=−8 to 8 for both the laser and LED sources.

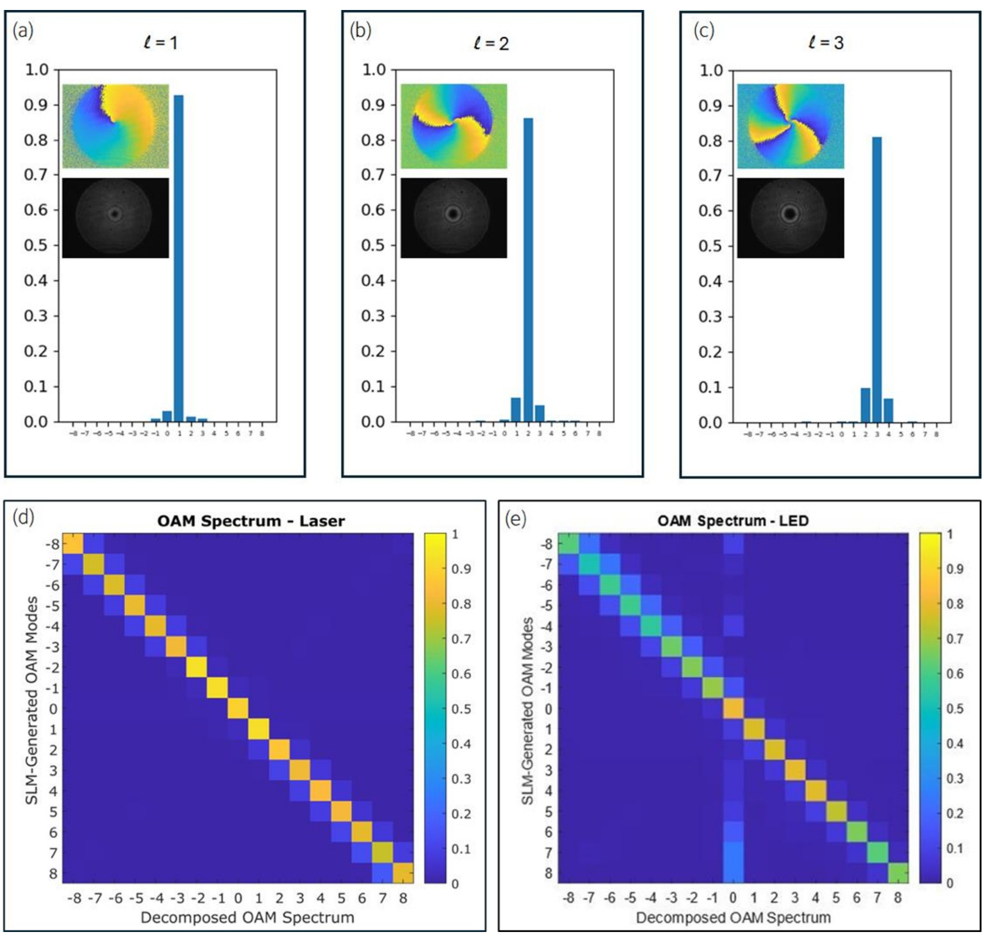

Fig. 2. OAM beam generation and purity analysis. (a)–(c) Recovered phase of the OAM beams for ℓ= 1,2,3, captured using a 5-step interferometric phase retrieval method. (d)–(e) OAM spectra for the laser and LED sources for ℓ=−8 to 8.

A comparison between Figures 2(d) and 2(e) reveals that the laser source generates purer modes compared to the LED. Although the diagonal signal in Figure 2(e) indicates that the correct modes are being generated, there is a higher unmodulated component in the LED case, particularly a larger signal at ℓ=0 when compared. This discrepancy arises because the SLM is calibrated for the central wavelength, leading to a less precise modulation across the LED spectrum. It would be interesting to explore whether calibrating the SLM based on the source spectrum could reduce the unmodulated component in the LED case. This could be achieved by directly measuring the OAM during the calibration process, rather than calibrating gray values from phase shifts, as in traditional calibration methods.

4 Conclusions

In this work, we explored the integration of OAM with classical OCT. We demonstrated the generation of OAM modes with high purity in an OCT-compatible setup. The purity of these modes was quantified through phase retrieval and OAM spectrum decomposition. Using a broadband source, we observed a decrease in mode purity, manifested as an unmodulated zero-order component in the OAM spectra. However, the dominant component still corresponds to the correctly generated OAM mode. Our preliminary results demonstrate the potential of incorporating OAM as an additional degree of freedom in OCT. In the future, we aim to leverage the OAM basis for noise filtering to enhance OCT performance. Furthermore, this work can be extended to quantum OCT, where OAM entanglement is inherently integrated into the SPDC photon generation process.

Funding. Horizon Europe Framework Programme for Research and Innovation, SEQUOIA project (101070062).

References

1. M. Figuras, J. Robaszkiewicz, and J. Wierzbowska, "Optical coherence tomography in imaging of macular diseases," *Klinika Oczna/Acta Ophthalmologica Polonica* 112.2 (2010). eISSN: 2719-3209
2. M. E. Brezinski, "Capabilities, limitations, and misconceptions of using OCT to assess vulnerable plaques," *Nature Reviews Cardiology*, (2014), doi: 10.1038/NRCARDIO. 2014.62-C
3. M. Okano, H. Lim, R. Okamoto, *et al.* "0.54 μm resolution two-photon interference with dispersion cancellation for quantum optical coherence tomography," *Sci Rep* **5**, 18042, (2016). doi :10.1038/srep18042
4. M. C. Teich, M. B. Nasr, A. V. Sergienko, and B. E. A. Saleh, "Entangled-Photon Optical Coherence Tomography," *Coherent Optical Technologies and Applications* (2006). doi: 10.1364/COTA.2006.CWD2
5. A. Mair, A. Vaziri, G. Weihs, and A. Zeilinger, "Entanglement of the orbital angular momentum states of photons," *Nature*, (2001), doi: 10.1038/35085529
6. R. Fickler *et al.*, "Entanglement of very high orbital angular momentum," *Laser Science* (2011). doi: 10.1364/LS.2011.LTHC1
7. N. Biton, J. Kupferman, and S. Arnon, "OAM light propagation through tissue.," *Scientific Reports*, (2021), doi: 10.1038/S41598-021-82033-6
8. S. Hell and J. Wichmann, "Breaking the diffraction resolution limit by stimulated emission: stimulated-emission-depletion fluorescence microscopy," *Opt. Lett*. 19, 780-782 (1994). doi: 10.1364/OL.19.000780